Study of Mercury [Hg(II)] Adsorption from Aqueous Solution on Functionalized Activated Carbon

Oscar D. Caicedo Salcedo, Diana P. Vargas, Liliana Giraldo, and Juan Carlos Moreno-Piraján*
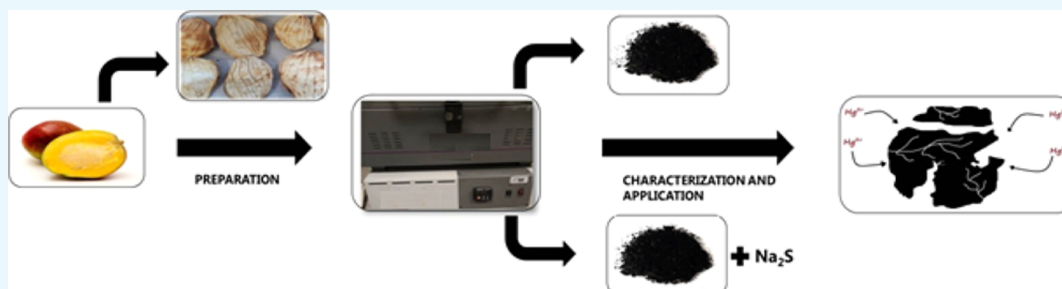
Cite This: *ACS Omega* 2021, 6, 11849−11856

Read Online

ACCESS | Metrics & More | Article Recommendations

ABSTRACT: Mercury and its compounds are toxic substances, whose uncontrolled presence in the environment represents a danger to ecosystems and the organisms that inhabit in it. For this reason, in this work, we carried out a study of mercury [Hg(II)] adsorption from aqueous solution on functionalized activated carbon. The activated carbons were prepared by chemical activation of a mango seed with solutions of $CaCl_2$ and H_2SO_4 at different concentrations, later, the carbonaceous materials were functionalized with Na_2S, with the aim of increasing the sulfur content in the carbonaceous matrix and its affinity to mercury. The materials were characterized using: proximal analysis, scanning electron microscopy, Boehm titrations, point zero charge (pH_{PZC}), and infrared spectroscopy. Additionally, immersion calorimetries were performed in the mercury solution. The results of textural and chemical characterization show materials with low Brunauer−Emmett−Teller (BET) surface areas between 2 and 33 $m^2 \cdot g^{-1}$ and low pore volumes. However, they had a rich surface chemistry of oxygenated groups. The enthalpies of immersion in the mercury solutions are between −31.71 and −77.31 $J \cdot g^{-1}$, showing a correlation between the magnitude of the enthalpic data and the adsorption capacity of the materials. It was evidenced that the functionalization process produces a decrease in the surface area and pore volume of the activated carbons, and an increase in the sulfur content of the carbonaceous matrix. It was evidenced that the functionalization process generated an increase in the mercury [Hg(II)] adsorption capacity between 21 and 49% compared to those of the nonfunctionalized materials, reaching a maximum adsorption capacity of 85.6 $mgHg^{2+}g^{-1}$.

1. INTRODUCTION

While the contaminating power of heavy metals is widely known, it is worth mentioning that in this group of elements, many of them are naturally found and even some of them are biologically important, fulfilling roles such as micro and macronutrients, catalysts of biological reactions, and even essential molecules for life such as hemoglobin and hemocyanin that have iron and copper in their molecular structure, respectively.[1,2] The problem is that the pollutant emissions derived from human activities have increased the natural concentrations of these metals to highly toxic and dangerous levels.[2]

Because of the demand for products and the increase in industries, the exploitation and use of heavy metals have intensified exponentially, generating an increase in the metal ion production that, at high concentrations, are toxic to ecosystems such as Ni(II), Cd(II), Pb(II), and Hg(II) among others.[3] The high demand for products, especially certain

metals such as gold, extracted by mining, has caused serious damage to ecosystems because of the release of heavy metals such as arsenic and mercury.[3,5,6]

Mercury and its compounds, especially organomercuric species, are related to various diseases and cause damage to organisms where they accumulate, from bacteria and small organisms to mammals and humans. In this sense, organic compounds such as methylmercury have the highest levels of toxicity.[5−7] Thus, in fish and other mammals, mercury more precisely in its methylated form (CH_3Hg^+) tends to pass through the intestinal wall when ingested, and accumulates in

the muscle tissue, thus generating the phenomenon of biomagnification. In humans, methylmercury is associated with different biological damage such as a congenital lesion, teratogenic and carcinogenic effects, gastroenteritis, ataxia, loss of vision, and it directly affects fetal development in humans.[3,5,7]

There are a lot of technological alternatives used for environmental decontamination, which allow mitigation of the anthropic impact generated on ecosystems. Techniques such as reverse osmosis, coagulation, electrochemistry, ion exchange, catalysis, and adsorption have been proposed to solve these contamination problems; adsorption being one of the most used and booming techniques because of its characteristics such as versatility, low cost, specificity, and efficiency in decontamination processes.[8]

Activated carbons are a group of highly porous materials that are obtained by the reaction of a carbonized material with oxidizing gases or by the carbonization of "activated" lignocellulosic precursors with different types of chemical agents.[9,10] It is widely known that surface chemistry is an important parameter to consider in activated carbons because of the different chemical or specific interactions that can be generated between the adsorbate and the adsorbent, without neglecting other characteristics that the materials may have, such as their acidic or basic surface and their catalytic properties among others.[9−12]

The surface chemistry of activated carbons can be very diverse depending on the activating agent used in the preparation process.[9] Because of their structure, on the surface of activated carbons we can find different oxygenated chemical groups such as carboxylic acids, lactones, phenols, ethers, carbonyls, or pyrones, additionally, it is also possible to find heteroatoms in the basal planes of their structure such as nitrogen, phosphorus, chlorine or sulfur, and delocalized π electrons.[9−16]

While the porosity of these materials is a characteristic that makes them useful and striking to be used in adsorption, this is not enough to ensure that the adsorption process is carried out efficiently. In general, several studies have shown[16−18] that the appropriate modification of their surface chemistry is a useful strategy to improve the interaction capacity between the adsorbent and the adsorbate of interest.[4]

According to González-Gaitán et al.,[16] the modification of the surface chemistry of carbonaceous materials makes it possible to adapt their adsorbent and catalytic properties to improve their performance in different applications. Covalent chemical functionalization consists in the addition of different heteroatoms or molecules to the surface of the material by impregnating with solutions or gases containing the elements of interest; among the most used to functionalize activated carbons are elements such as phosphorus (P), nitrogen (N), oxygen (O), and sulfur (S).[16] The literature reports that for the removal or decontamination of mercury, materials functionalized with sulfur groups (thiols, sulfoxides, and sulfones) or in the presence of sulfur on the surface significantly increase the adsorption of this metal.[17] To achieve this chemical functionalization, different methodologies are used, from mixing coal directly with elemental sulfur, to injecting or pyrolyzing with sulfur-containing gases such as sulfur dioxide (SO_2). Although this functionalization increases the adsorption capacities of activated carbons, it affects their surface area, which in most cases suffers a considerable decrease; however, it

has been shown that despite this reduction, the adsorption capacities can increase up to 80%.[17]

Therefore, the aim of this research was the study of mercury [Hg(II)] adsorption in the aqueous phase on carbonaceous materials with different textural, structural, and chemical characteristics that were obtained by chemical activation of a mango seed with solutions of $CaCl_2$ and H_2SO_4 at different concentrations and additionally they were functionalized with Na_2S (sodium sulfide) to increase their affinity to mercury [Hg(II)].

2. MATERIAL AND METHODS

2.1. Preparation of the Activated Carbons. A mango seed was collected from a fruit pulp processing plant located in Ibague, Colombia. The seed was cleaned before impregnation. Then, it was dried for two days in an oven at 363 K and then crushed using a manual crusher to obtain a mixture of the three parts of the seed (endocarp, tegument, and kernel) with a maximum size of 2 cm (Figure 1).

Figure 1. Mango seed parts (endocarp, tegument, and kernel).

For all prepared samples, the impregnation of the mango seed was carried out at a ratio of 2 mL of solution/1 g of the precursor.[14] For the impregnation of the precursor, two activating agents were used: sulfuric acid (15% v/v) and calcium chloride (7% w/v). The mango seed mixture was impregnated with the said solutions for 48 h at a temperature of 358 K.

The carbonization was carried out in a Carbolite transverse furnace, in an N_2 atmosphere with a flow of 80 cm^3·min^{-1} with a heating ramp of 1 K·min^{-1}, up to a temperature of 723 K, having a residence time of 2 h. Once the carbonization was finished, the materials obtained were washed with hot distilled water until a neutral pH was obtained. The materials activated with calcium chloride were subjected to a wash with HCl prior to washing with hot distilled water, in order to remove traces of the activating agent.

The samples obtained were denoted: CAC7 (activated carbon with 7% p/v calcium chloride solution) and CAS15 (activated carbon with 15% v/v sulfuric acid solution).

2.2. Functionalization of the Activated Carbons. In order to increase the affinity of the carbonaceous materials obtained to the pollutant of interest, in this project Hg(II), the carbonaceous solids that were activated with the H_2SO_4 and $CaCl_2$ solutions were functionalized. To perform the functionalization, a solution of sodium sulfide Na_2S was prepared with a ratio of 1 g Na_2S/100 mL $-H_2O$ per gram of carbon. 20 g of carbon per sample was impregnated in the 100 mL of the Na_2S solution for 24 h at a temperature of 473 K. Once the impregnation time was completed, the two materials were washed with distilled water until constant pH was reached and then dried in an oven at 350 K.

The samples obtained were denoted: CAC7-S (CAC7+ Functionalization) and CAS15-S (CAS15+ Functionalization).

2.3. Characterization. Adsorbent materials were characterized using different experimental techniques. The surface morphologies of the prepared adsorbents were investigated by scanning electron microscopy−energy-dispersive X-ray spectroscopy (SEM−EDX) (JEOL, JSM-6490 LV EOL.). The chemical characterization was realized with different techniques. The proximate analysis was carried out according to the ASTM standard, using the test methods ASTM-D3173 for moisture, ASTM-D3174 for ashes, and ASTM-D3175 for volatile matter[19−21] (Hitachi Thermal Analysis System STA7200). Point zero charge (pH_{PZC}) was determined with the mass titration method proposed by Noh and Schwarz[22] using 0.05−0.6 g of the adsorbents in 30 mL of 0.1 M NaCl solution with an equilibrium time of 48 h at 298 K. A Boehm titration was carried out using 0.1 g of carbon and 50 mL NaOH, HCl, Na_2CO_3, and 0.1 M $NaHCO_3$ solutions.[16] The equilibrium time was 48 h at 298 K. Also, the information about the functional groups was obtained using Fourier transform infrared (FT-IR) spectroscopy (Shimadzu FT-IR Tracer-100). In addition, to understand the chemical interaction between the material and the pollutant, we realized immersion enthalpies in the mercury solution (150 mg·L^{-1}) using a homemade Tian-type calorimeter. The procedure to obtain the enthalpy of immersion consists of placing 10 mL of the solvent in a metal cell. In the heat reservoir of the calorimeter at 298 K; the calorimeter registers the output of electric potential as long as it has reached a baseline over time. Then, 100 mg of the activated carbon sample is placed in a glass vial and the immersion is performed.[15] If the immersion was satisfactory and the baseline is obtained again, the electrical calibration is performed. The variation of the electric potential versus time was used for the calculation of the immersion enthalpy.

Finally, textural characterization was determined with nitrogen sorption measurements N_2/77 K using Autosorb IQ2, Quantachrome Instruments (Boynton Beach, FL, USA).

2.4. Mercury Adsorption. For adsorption experiments, solutions of Hg(II) were made using an analytical grade reagent ($HgCl_2$), acquired from commercial houses, Merck Colombia, using distilled water as the solvent. The pH of the prepared solutions was adjusted to a value of 5 using 0.1 M solutions of NaOH and HCl to ensure the availability of metal ions based on pH induced by chemical speciation, which has been reported in previous studies.[23,24] For the determination of the concentration of the solutions from the calibration curves, an adsorption atomic absorption spectrophotometer (Thermo Scientific iCE 3500) connected to a generator of hydrides (Thermo Scientific VP100) was used. Mercury adsorption tests were carried out using a simple Batch adsorption system, based on what was proposed by different authors for adsorption of metal ions.[26−28] Simple solutions of Hg(II) metal ions were prepared in a concentration range of 10 to 150 mg·L^{-1}. In amber containers, 100 mg of activated carbon was contacted with 30 mL of each prepared solution, at an equilibrium time of 48 h at room temperature,[29] and constant stirring. Then, the solutions were filtered with Munktell Ahlstrom 391 filter paper to remove the activated carbon.

Finally, the obtained experimental data were modeled with the Freundlich and Langmuir equations. In the Freundlich model (eq 1), K_f is a constant that indicates the relative adsorption capacity of the adsorbent and n is a constant that refers to the intensity of the adsorption.[26]

$$Q_e = K_f Ce^{1/n} \tag{1}$$

In the Langmuir model (eq 2), Q_e is the amount of solute adsorbed per unit weight of the adsorbent at equilibrium, Ce is the concentration at equilibrium, Q_m is the maximum capacity of adsorption, and b is the constant related to the adsorption free energy.[26]

$$Q_e = \frac{K_l Ce}{1 + \alpha_L Ce} \tag{2}$$

The adjustment parameters of the models were calculated using the Rosenbrock Quasi-Newton optimization method, included in the STATISTICA software.

3. RESULTS AND DISCUSSION

3.1. Adsorbent Characterization. *3.1.1. Proximate Analysis.* The materials obtained have characteristics that are consistent with other materials prepared from lignocellulosic residues.[14,28,30] It is observed that the humidity percentage for most materials is between 8.2 and 28.4%. This is associated with the amount of water molecules that the material can retain when it is in contact with the environment. It is notable that CAC7-S presented a significant increase in humidity because the functionalization process generated a higher content of oxygenated groups that favor interaction with the water present in the environment.

The content of volatile matter was between 29 and 39.4%, which indicates that the activation and carbonization processes did generate changes in the amount of volatile matter in the precursor, and proximal analyses of the raw mango seed suggest the contents of volatile matter to be between 74 and 75%.[31] About the percentage of ash, it is observed that the values are not high for any of the carbons obtained, comparing the results with those of other lignocellulosic precursors where ash levels are up to 26%.[14,32] There is also evidence for an increase in the ash content in the activated carbons, which may be related to the functionalization process, because the agent did not react with the surface of the carbons, contributing to the inorganic matter content (Table 1).[31] On the other hand,

Table 1. Proximate Analysis of Activated Carbons

sample	proximate analysis			
	moisture	volatile matter	ash	fixed carbon
Endocarp[31]	4.3	75.8	0.6	19.3
Kernel[31]	2.3	74	1.1	22.6
CAC7	8.2	29	0.9	61.9
CAS15	8.2	32	1.4	58.4
CAC7-S	28.4	39.4	6.4	25.8
CAS15-S	11	36.5	6.1	46.4

the fixed carbon content in all the materials was higher than the values reported for the precursor. However, the functionalized materials contained the lowest amount of fixed carbon, this is associated with the impregnation process with sodium sulfide and the oxidation reactions in the matrix of the material.

3.1.2. Scanning Electron Microscopy. Figure 2 presents the microphotographs obtained for the samples prepared in this study. It is possible to observe a porous network made up of access channels to the carbonaceous matrix of solids, which
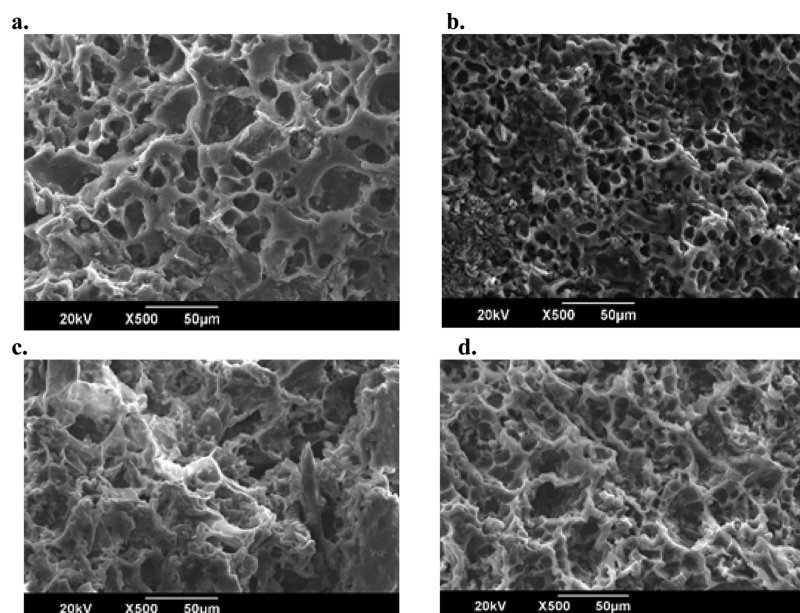
Figure 2. SEM images: (a) CAC7; (b) CAS15; (c) CAC7-S; and (d) CAS15-S.

shows the degradation of the precursor caused by the chemical activation process. Making a comparison between non-functionalized and functionalized materials, a structural change in the porosity generated by the reaction between the activated carbons and the agent used in the chemical modification was found. That reaction could cause a degradation of the carbonaceous material or its reorganization, which is reflected in the decrease in surface area and pore volume. Some of the images of the activated carbons are similar to other microphotographs that have been taken using other activated carbons prepared from the mango seed, such as those obtained by Somayajula et al.[27] and Rai et al.[28]

3.1.3. Isotherm Determination of N_2 Adsorption–Desorption at 77K. Table 2 presents the textural character-

Table 2. Analysis of S_{BET}

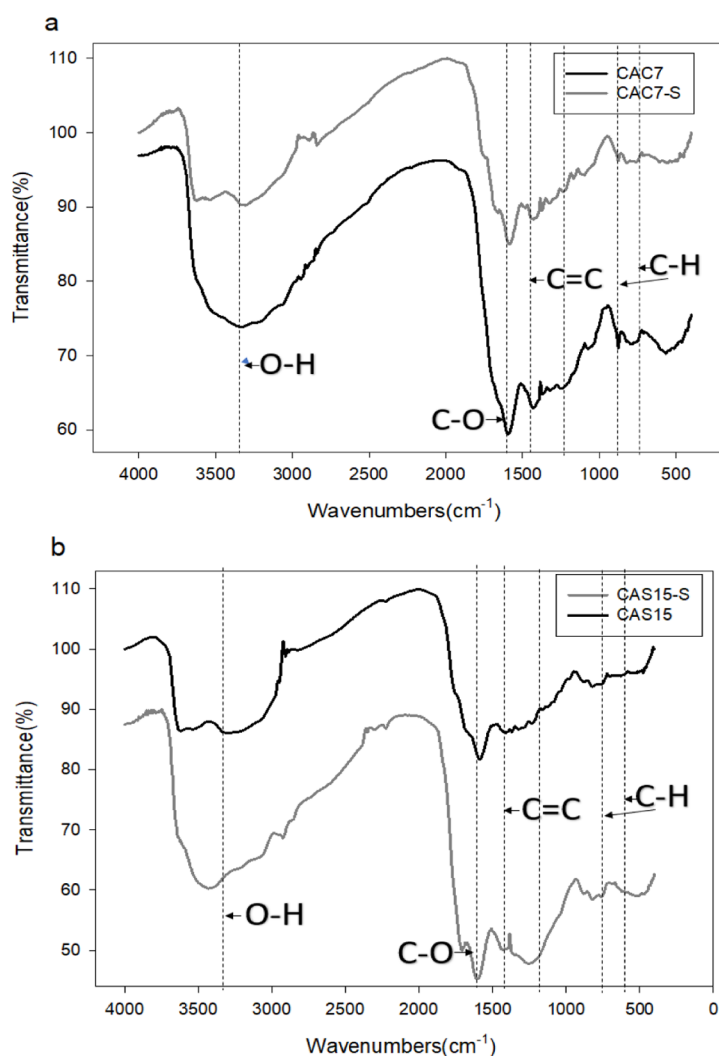| sample	S_{BET} ($m^2 \cdot g^{-1}$)	V_0 ($cm^3 \cdot g^{-1}$)
Precursor	1	0.0003
CAC7	33	0.019
CAS15	12	0.006
CAC7-S	25	0.014
CAS15-S	2	0.0007

istics of the precursor and the activated carbons. We obtained surface areas between 2 and 33 $m^2 \cdot g^{-1}$ and pore volumes between 0.0007 and 0.019 $cm^3 \cdot g^{-1}$, these parameters are low compared to those of other carbons obtained using the activated mango seed, whose areas range are from 400 to 920

$m^2 \cdot g^{-1}$.[27,28,33] However, the increase in the BET area and the pore volume in the precursor with the activation process is evident, showing better results when $CaCl_2$ is used. The attack of this activating agent is less than that produced with H_2SO_4, which is a strong dehydrating agent that breaks down the components of the lignocellulosic material, even leading to a collapse of the structure, generating a smaller area and a less pore volume in the carbons.[34−37] Likewise, a decrease in these parameters is observed because of the functionalization process. This result coincides with what can be observed in the microphotographs.

3.1.4. Boehm Titration and pH_{PZC} Determination. In Table 3, the results of the Boehm titration and the determination of the point zero charge of each material are shown. All the prepared activated carbons have a variety of oxygenated groups on the surface; the content varies depending on the concentration of the activating agent used in the preparation of the solids and the functionalization process. Activation and functionalization processes generate surface groups richer in surface chemistry, which is related to the concentration of the activation agent. Because of the greater degradation of the precursor, the carbonaceous materials generated have a greater amount of carbon atoms with unsaturated valences, in the basal planes of the graphene sheets. When these groups interact with the oxygen in the environment, they give rise to groups such as carboxylics, lactonics, and phenolics among others. The functionalized materials (CAC7-S and CAS15-S) increased the values of total acidity by 57 and 90%, respectively, as well as the content of phenolic groups.[16] The increase in the acidity of the materials can be explained by the fact that in the

Table 3. Surface Chemistry Characterization (Boehm Titration) and pH_{PZC}

sample	carboxylic groups ($mmol \cdot g^{-1}$)	lactone groups ($mmol \cdot g^{-1}$)	phenolic groups ($mmol \cdot g^{-1}$)	total acidity ($mmol \cdot g^{-1}$)	total basicity ($mmol \cdot g^{-1}$)	pH_{PZC}
CAC7	0.305	1.318	3.852	2.840	1.739	6.7
CAS15	0.500	0.219	2.142	2.424	0.365	5.4
CAC7-S	0.512	0.047	4.021	4.485	0.215	6.3
CAS15-S	0.335	0.081	4.355	4.608	0.127	5.5

Figure 3. FT-IR spectra of (a) CAC7/CAC7-S and (b) CAS15/CAS15-S.

functionalization process of the carbons, the carbonaceous matrix is enriched with sulfur atoms, giving rise to sulfur groups such as sulfones or sulfoxides, among others.[16,25] These groups cannot be specifically identified or measured by Boehm titration, but contribute to the quantification of the total acidity of the adsorbent materials. This result is of interest and relevance, taking into account that the enrichment of the chemical surface with sulfur atoms will allow a greater affinity of the activated carbons for mercury $[Hg(II)]$. For all the activated carbons, a higher total acidity was obtained compared to the total basicity; therefore, the character of the surface is acidic as evidenced by a pH_{PZC} less than 7.

3.1.5. FTIR Spectra and EDX. The FTIR spectra of the carbons prepared from the mango seed are shown in Figure 3. Figure 3a shows the spectra obtained for samples CAC7 and CAC7-S. There is a large band at 3300 cm^{-1}, which is associated with stretching of the (−OH) group, characteristic of phenolic and carboxylic groups. Additionally, the thickness of the band also indicates the presence of moisture in the sample, which can be observed in all the spectra obtained for different activated carbons. For all the materials, two defined peaks were found at 1600 and 1400 cm^{-1}, these peaks are associated with the C═C bonds, which are characteristic of activated carbons because they correspond to the bonds that make up the graphene sheets. Besides, between 760 and 890

cm^{-1} is observed for all the samples, a small band related to the out-of-plane aromatic C−H vibrations. Moreover, it is possible to identify a band of different intensity located between 900 and 1450 cm^{-1}, in this region it is difficult to assign the bands with certainty because there is an overlap of the C−O stretching of different surface groups.[27]

Figure 3b shows the spectra of CAS15 and CAS15-S. These spectra have the same bands as mentioned above. However, it is observed that the CAS15-S material has a more defined peak at 1300 cm^{-1}. In this region, certain sulfur-related bonds such as those of sulfones and sulfonic acid can be found. There is a possibility that the sulfur-related bonds overlap in the 1300 and 1550 cm^{-1} region. Therefore it is not possible to conclude using this technique, the specific presence of the said compounds.[17] Nevertheless, the EDX analysis showed that the functionalization process of the sample was activated with $CaCl_2$, incorporating sulfur into the carbonaceous matrix of the material because it was not initially present, while in the sample activated with H_2SO_4, sulfur is present in triplicate in activated carbons.

3.2. Mercury Ion Removal from the Aqueous Phase. The results of mercury adsorption from the aqueous solution were adjusted to the Langmuir and Freundlich models. Figure 4 presents the experimental isotherms of adsorption of the Hg(II) metal ion in the aqueous phase for CAS5 and CAS15.
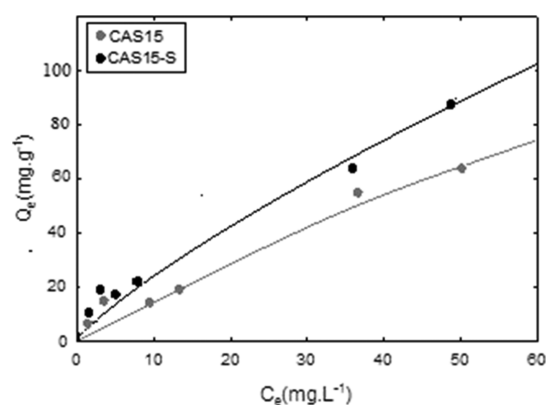
Figure 4. Adsorption isotherms of the Hg(II) metal ion in the aqueous phase of CAS15 and CAS15-S. The lines represent the best-fitting model (Freundlich) obtained in this study.

Also, it shows the representation of the Freundlich model in which the samples presented the best fit. Each isotherm shows the maximum adsorption capacity of the Hg(II) metal ion, that the prepared materials have, obeying the following order CAS15-S (85.6 mg·g^{-1}) > CAS15 (57.3 mg·g^{-1}).

Table 4 presents the results of the mercury adsorption tests, also with the adjustment parameters of the applied Langmuir and Freundlich models. We obtained maximum adsorption capacity between 57.3 and 85.6 mgHg^{2+}·g^{-1} of carbon, the differences between the adsorption capacities of the Hg(II) metal ion of the carbonaceous materials indicate that the chemical and textural characteristics of the porous solids influenced directly the adsorption process. The materials with the most abundant surface chemistry (CAC7-S and CAS15-S) exhibited the highest values of the maximum adsorption capacities, indicating that the functionalization process increased the affinity of the materials for the Hg(II) metal ion. The increase in this adsorption capacity is attributed to the appearance of different functional sulfur groups such as sulfones, sulfoxides, sulfides, among others, which allow the formation of different complexes between the metal ion and sulfur.[23,25,29] Madhava et al.[36] also relate this increase in adsorption capacity to Pearson's theory of hard acids/hard bases and soft acids/soft bases. In the mercury speciation diagram shown in other studies,[24] it is possible to observe the Hg(II) metal ion at pH used for adsorption tests, it behaves like a soft acid, which would be attracted to soft bases, such as the sulfur groups present on the surface of the carbons. This would allow the formation of Hg(HS)$_2$ complexes or other chemical processes such as the H$^+$ ion exchange of the other functional groups.

On the other hand, it can be seen that the adsorption data fit the values of R^2 between ($0.982-0.995$) obtained using the Freundlich model. The fit of the materials to this model

suggests that the activated carbons have a heterogeneous surface and the adsorption of the Hg(II) metal ion is in multilayer, in others studies the multilayer adsorption of metal ions is associated with the electrostatic interaction between metal ions and the negatively charged functional groups (such as −COO−, −OH, and −SH) on the adsorbent. The formation of the metal−sulfur complex through ion-exchange and electrostatic interactions is considered to be the plausible mechanistic approach for metal-ion adsorption.[11,17,18,23,25,29] In addition, the results for parameter $N > 1$ for activated carbons adjusted to the Freundlich model demonstrate a favorable adsorption in the four samples and an increase in the affinity between the materials and the Hg(II) metal ion with the functionalization process. Likewise, it is possible to observe a higher K_f value in the functionalized carbons that indicates a greater mercury adsorption capacity (Q_e), this is related to the increase in surface chemistry of materials and the presence of functional groups with sulfur, demonstrating that these groups play an important role in the adsorption of the Hg(II) metal ion.

Moreover, Table 4 shows the values obtained for the enthalpies of immersion of the materials in 150 mg·L^{-1} mercury solution, which are between -31.71 J·g^{-1} and -77.31 J·g^{-1}. The results show a correlation between the enthalpic values and the adsorption capacity of carbonaceous materials, and it was found that the energy associated with the process increases as the amount of adsorbate retained increases. It is important to say that the enthalpic values obtained do not reach the order of the chemical bond ($200-500$ kJ·mol^{-1}), therefore, it is inferred that the adsorption phenomena presented in the systems would be related to physisorption processes.[40−42]

Finally, the adsorption results obtained in this study were compared with other adsorption capacities reported by other authors (Table 5). As it is observed under different conditions of different studies, the concentrations range between 10 mgHg^{2+} g^{-1} and 200 mgHg^{2+}·g^{-1} upon adjusting the pH of the solutions to 5 or close to this value. Contrasting the adsorption results of the other activated carbons obtained with more efficient treatments, the values obtained for the activated carbons in this study are lower with capacities greater than 100 mgHg^{2+}·g^{-1}; however, the capacities of carbons obtained in this study exceed the capacities reported by Madhava et al.,[36] Kannan and Sugantha,[37] among others.

The highest Hg(II) metal ion adsorption capacities are evidenced in porous materials that were subjected to sulfur functionalization processes.[17] This demonstrates that the surface enrichment of activated carbons with different functional groups related to sulfur can provide better results in the decontamination of that metal in aqueous solution.[39]

Table 4. Maximum Adsorption Capacity of Hg(II) Metal Ion, Immersion Enthalpies in Mercury Solution at 150 mg·L^{-1}, and Adsorption Parameters of the Models Applied

			Langmuir			Freundlich		
sample	Q_e (mg·g^{-1})	$-\Delta H_{imm}$ Hg^{2+} (J·g^{-1}) (150 mg·L^{-1})	Q_o	K_L	R^2	K_F	N	R^2
CAC7	56.1	33.39 ± 0.4	79.11	0.007	0.903	3.35	1.236	0.982
CAS15	57.3	31.71 ± 0.6	74.45	0.041	0.905	4.67	1.525	0.995
CAC7-S	70.3	63.60 ± 1.5	124.13	0.032	0.910	6.32	1.489	0.993
CAS15-S	85.6	77.31 ± 0.5	92.16	0.040	0.925	6.90	1.576	0.987

Table 5. Comparison between Hg(II) Adsorption Capacity of Different Activated Carbons in Different Reports

adsorbent	conditions	Q_O	refs
activated carbon impregnated with sulfur	pH 5,5 1−105 mg·L^{-1}	800 mg·g^{-1}	[23]
activated carbon from organic sewage sludge, activated with H_2SO_4, H_3PO_4, and $ZnCl_2$.	pH 5 10−200 mg·L^{-1}	128 mg·g^{-1}	[24]
activated carbon doped with nitrogen and sulfur.	pH 4−6 10−200 mg·L^{-1}	511.78 mg·g^{-1}	[25]
activated carbon with $ZnCl_2$ from mango kernel.	pH 6,5 10−50 mg·L^{-1}	19.7 mg·g^{-1}	[27]
activated carbon prepared from *ceiba pentandra* helmets, *Phaseolus aureus* helmets, and residues from *Cicer arietino*.	pH 2−9 10−140 mg·L^{-1}	25.88 mg·g^{1} 23.66 mg·g^{-1} 22.88 mg·g^{-1}	[36]
commercial activated carbon and prepared nuts.	pH 6 25−175 mg·L^{-1}	24.8 mg·g^{-1}	[37]
activated carbon with H_2SO_4 and $(NH_4)_2S_2O_8$ from Sago waste.	pH 5 20−50 mg·L^{-1}	55.6 mg·g^{-1}	[38]
activated carbon from mango seed activated with H_2SO_4 and $CaCl_2$, functionalized with sodium sulfide (Na_2S)	pH 5 10−150 mg·L^{-1}	85.6 mg·g^{-1}	in this work

4. CONCLUSIONS

Macromesoporous materials were successfully prepared using the mango seed as a precursor material. Although the materials have low surface areas between 2 and 33 m^2·g^{-1}, they have abundant surface chemistry of oxygenated groups such as carboxyls and phenols, which are important for their application in systems of metal ion adsorption. Nevertheless, the functionalization process affected the textural characteristics of the materials,[43] considerably reducing their areas; however, functionalization also generated an increase in the number of surface groups, which are directly related to the adsorbent capacities of the obtained materials.

On the other hand, the maximum adsorption capacity of mercury ranged between 57.3 and 85.6 mgHg^{2+}·g^{-1}. The functionalization processes are very important for the improvement of the adsorbent capacities of activated carbons because despite a reduction in their textural characteristics, better results were obtained for the adsorption process of the Hg(II) metal ion. This is reflected as an increase between 21 and 49% compared to those of nonfunctionalized materials. Moreover, the presence of heteroatoms with sulfur and an increase of the oxygenated groups on the surface could generate an increase in the adsorption capacity of the materials. The adjustment of the Freundlich model for adsorption processes of this study suggests a heterogeneous surface with different sites of interaction between carbon and the metal ion, which contrasts with the results obtained during the characterization of the materials. Finally, adsorption system conditions such as pH and equilibrium time, along with the chemical characteristics of materials such as pHpzc and the abundance of surface groups or heteroatoms turn out to be the most important parameters to achieve good adsorption systems of Hg(II) ions from aqueous solution.

■ AUTHOR INFORMATION

Corresponding Author

Juan Carlos Moreno-Piraján − *Facultad de Ciencias, Departamento de Química, Grupo de Investigación en Sólidos Porosos y Calorimetría, Universidad de los Andes, Bogotá 111711, Colombia;* ⊙ orcid.org/0000-0001-9880-4696; Phone: (571) 3394949 Ext. 3465; Email: jumoreno@uniandes.edu.co

Authors

Oscar D. Caicedo Salcedo − *Facultad de Ciencias, Departamento de Biología, Grupo de Investigación en Materiales Porosos con Aplicaciones Tecnológicas y Ambientales, Universidad del Tolima, Ibagué 730006299, Colombia*

Diana P. Vargas − *Facultad de Ciencias, Departamento de Química, Grupo de Investigación en Materiales Porosos con Aplicaciones Tecnológicas y Ambientales, Universidad del Tolima, Ibagué 730006299, Colombia*

Liliana Giraldo − *Facultad de Ciencias, Departamento de Química, Grupo de Investigación en Calorimetría, Universidad Nacional de Colombia, Bogotá 111321, Colombia*

Complete contact information is available at:
https://pubs.acs.org/10.1021/acsomega.0c06084

Notes
The authors declare no competing financial interest.

■ ACKNOWLEDGMENTS

■ REFERENCES

(1) Bolan, N. S.; Choppala, G.; Kunhikrishnan, A.; Park, J.; Naidu, R. Microbial transformation of trace elements in soils in relation to bioavailability and remediation. In . *Reviews of Environ.l Contam. and Toxicol*; Whitacre, M. D., Ed. Springer, New York, NY, 2013; pp. 1−56.

(2) Adriano, D. C.; Wenzel, W. W.; Vangronsveld, J.; Bolan, N. S. Role of assisted natural remediation in environmental cleanup. *Geoderma* **2004**, *122*, 121−142.

(3) Vareda, J. P.; Valente, A. J. M.; Durães, L. Assessment of heavy metal pollution from anthropogenic activities and remediation strategies: A review. *J. Environ. Manage.* **2019**, *246*, 101−118.

(4) Cai, J. H.; Jia, C. Q. Mercury removal from aqueous solution using Coke-Derived sulfur-impregnated activated carbons. *Ind. Eng. Chem. Res.* **2010**, *49*, 2716−2721.

(5) Morton-Bermea, O.; Jiménez-Galicia, R. G.; Castro-Larragoitia, J.; Hernández-Álvarez, E.; Pérez-Rodríguez, R.; García-Arreola, M. E.; Gavilán-García, I.; Segovia, N. Anthropogenic impact of the use of Hg in mining activities in Cedral S.L.P. Mexico. *Environ. Earth Sci.* **2015**, *74*, 1161−1168.

(6) Naharro, R.; Esbrí, J. M.; Amorós, J. A.; Higueras, P. L. Experimental assessment of the daily exchange of atmospheric mercury in *Epipremnum aureum*. *Environ. Geochem. Health* **2020**, *42*, 3185−3198.

(7) Londoño Franco, L. F.; Londoño Muñoz, P. T.; Muñoz Garcia, F. G. Los riesgos de los metales pesados en la salud humana y animal. *Biotecnol. Sect. Agropecu. Agroind.* **2016**, *14*, 145−153.

(8) Fu, F.; Wang, Q. Removal of heavy metal ions from wastewaters: a review. *J. Environ. Manage.* **2011**, *92*, 407−418.

(9) *Chemistry and Physics of Carbon*; Radovic, L. R., Ed.; Marcel Dekker, Inc.: New York, 2000; Vol. *27*; pp 24−35.

(10) Vargas, D. P.; Giraldo, L.; Ladino, Y.; Moreno, J. C. Síntesis y caracterización de monolitos de carbón activado utilizando como precursor cáscara de coco. *Afinidad* **2009**, *66*, 38−43.

(11) Martín, M. J. *Adsorción física de gases y vapores por carbones*; Universidad de Alicante (Publicaciones): Alicante. España, 1988; pp 27−30.

(12) Worch, E. *Adsorption technology in water treatment*; Walter de Gruyter GmbH & Co: Berlin, Germany, 2012; pp 332.

(13) Ioannidou, O.; Zabaniotou, A. Agricultural residues as precursors for activated carbon production-A review. *Renewable Sustainable Energy Rev.* **2007**, *11*, 1966−2005.

(14) Acevedo, S.; Giraldo, L.; Moreno-Piraján, J. C. Caracterización textural y química de carbones activados preparados a partir de cuesco de palma africana (Elaeis guineensis) por activación química con CaCl₂ y MgCl₂. *Rev. Colomb. Quim.* **2015**, *43*, 18−24.

(15) Moreno-Piraján, J.; Giraldo, L.; García-Cuello, V.; Vargas-Delgadillo, D. P.; Murillo, Y.; Rodríguez, P.; Castillo, M. *Interaction thermodynamics between Gas-Solid and Solid-Liquid on carbon materials. Thermodynamics/Book 1*; INTECH. Rijeka, Croatia, 2011; pp 164−195.

(16) González-Gaitán, C.; Ruiz-Rosas, R.; Morallón, E.; Cazorla-Amorós, D. Modificación de la química superficial de los materiales carbonosos. Un aspecto clave para mejorar sus aplicaciones; Instituto Universitario de Materiales de Alicante. Boletín del Grupo Español del Carbón. 2017, *45*, 22−31.

(17) Hadi, P.; To, M.-H.; Hui, C.-W.; Lin, C. S. K.; McKay, G. Aqueous mercury adsorption by activated carbons. *Water Res.* **2015**, *73*, 37−55.

(18) Wajima, T.; Murakami, K.; Kato, T.; Sugawara, K. Heavy metal removal from aqueous solution using carbonaceous K2 S-impregnated adsorbent. *J. Environ. Sci.* **2009**, *21*, 1730−1734.

(19) *ASTM D3173/D3173M-17a. Standard Test Method for Moisture in the Analysis Sample of Coal and Coke*. ASTM International, West Conshohocken, PA, 2012.

(20) *ASTM D3174-12. Standard Test Method for Ash in the Analysis Sample of Coal and Coke from Coal*. ASTM International, West Conshohocken, PA, 2013.

(21) *ASTM D3175-17. Standard Test Method for Volatile Matter in the Analysis Sample of Coal and Coke*. ASTM International, West Conshohocken, PA, 2011.

(22) Noh, J. S.; Schwarz, J. A. Estimation of the point of zero charge of simple oxides by mass titration. *J. Colloid Interface Sci.* **1989**, *130*, 157−164.

(23) Wang, J.; Deng, B.; Wang, X.; Zheng, J. Adsorption of Aqueous Hg(II) by Sulfur-Impregnated Activated Carbon. *Environ. Eng. Sci.* **2009**, *26*, 1693−1699.

(24) Zhang, F.-S.; Nriagu, J. O.; Itoh, H. Mercury removal from water using activated carbons derived from organic sewage sludge. *Water Res.* **2005**, *39*, 389−395.

(25) Qin, H.; Xiao, R.; Guo, L.; Meng, J.; Chen, J. Mercury (II) adsorption from aqueous solution using nitrogen and sulfur co-doped activated carbon. *Water Sci. Technol.* **2017**, *2017*, 310−318.

(26) Rodríguez-Estupiñán, P.; Giraldo, L.; Moreno-Piraján, J. C. Modificación de la química superficial de carbones activados. Efecto de la oxidación con soluciones de HNO₃y H₂O₂ sobre la remoción de Cadmio (II) en solución acuosa. *Afinidad* **2014**, *71*, 49−56.

(27) Somayajula, A.; Aziz, A. A.; Saravanan, P.; Matheswaran, M. Adsorption of mercury (II) ion from aqueous solution using low-cost activated carbon prepared from mango kernel. *Asia-Pac. J. Chem. Eng.* **2012**, *8*, 1−10.

(28) Rai, M. K.; Shahi, G.; Meena, V.; Meena, R.; Chakraborty, S.; Singh, R. S.; Rai, B. N. Removal of hexavalent chromium Cr (VI) using activated carbon prepared from mango kernel activated with H₃PO₄. *Resour.-Effic. Technol.* **2016**, *2*, S63−S70.

(29) Asasian, N.; Kaghazchi, T.; Faramarzi, A.; Hakimi-Siboni, A.; Asadi-Kesheh, R.; Kavand, M.; Mohtashami, S.-A. Enhanced mercury adsorption capacity by sulfurization of activated carbon with SO2 in a bubbling fluidized bed reactor. *J. Taiwan Inst. Chem. Eng.* **2014**, *45*, 1588−1596.

(30) De Souza, T. N. V.; Vieira, M. G. A.; Da Silva, M. G. C.; Brasil, D. d. S. B.; de Carvalho, S. M. L. H3PO4-activated carbons produced from açai stones and Brazil nut shells: removal of basic blue 26 dye from aqueous solutions by adsorption. *Environ. Sci. Pollut. Res.* **2019**, *26*, 28533−28547.

(31) Elizalde-González, M. P.; Hernández-Montoya, V. Characterization of mango pit as raw material in the preparation of activated carbon for wastewater treatment. *Biochem. Eng. J.* **2007**, *36*, 230−238.

(32) Uçar, S.; Erdem, M.; Tay, T.; Karagöz, S. Preparation and characterization of activated carbon produced from pomegranate seeds by ZnCl2 activation. *Appl. Surf. Sci.* **2009**, *255*, 8890−8896.

(33) Dzigbor, A.; Chimphango, A. Production and optimization of NaCl-activated carbon from mango seed using response surface methodology. *Biomass Convers. Biorefin.* **2019**, *9*, 421−431.

(34) Molina-Sabio, M.; Rodríguez-Reinoso, F. Role of chemical activation in the development of carbon porosity. *Colloids Surf., A* **2004**, *241*, 15−25.

(35) Inbaraj, B.; Sulochana, N. Mercury adsorption on a carbon sorbent derived from fruit shell of *Terminalia catappa*. *J. Hazard. Mater.* **2006**, *133*, 283−290.

(36) Madhava, R. M.; Kumar, R. D. H. K.; Venkateswarlu, P.; Seshaiah, K. Removal of mercury from aqueous solutions using activated carbon prepared from agricultural by-product/waste. *J. Environ. Manage.* **2009**, *90*, 634−643.

(37) Kannan, N.; Sugantha, S. J. Removal of mercury (II) ions by adsorption onto dates nut and commercial activated carbons: A comparative study. *Indian J. Chem. Technol.* **2005**, *12*, 522−527.

(38) Kadirvelu, K.; Kavipriya, M.; Karthika, C.; Vennilamani, N.; Pattabhi, S. Mercury (II) adsorption by activated carbon made from sago waste. *Carbon* **2004**, *42*, 745−752.

(39) Boehm, H. P. Surface oxides on carbon and their analysis: a critical assessment. *Carbon* **2002**, *40*, 145−149.

(40) Murillo Acevedo, Y. S.; Morales Mancera, L. T.; Moreno-Piraján, J. C.; Flórez Vives, M. Regeneration of activated carbon by applying the phenolic degrading fungus Scedosporium apiospermum. *J. Environ. Chem. Eng.* **2020**, *8*, 103691.

(41) Moreno-Piraján, J. C.; Giraldo, L.; Gómez, A. A. Batch type heat conduction microcalorimeter for immersion heat determinations: design, calibration and applications. *Thermochim. Acta* **1998**, *290*, 1−12.

(42) Giraldo, L.; Huertas, J. I.; Valencia, A.; Carlos Moreno, J. A Heat Conduction Microcalorimeter for the Determination of the Immersion Heats of Activated Carbon into Phenol Aqueous Solutions. *Instrum. Sci. Technol.* **2003**, *31*, 385−397.

(43) Rehman, A.; Park, S.-J. Comparative study of activation methods to design nitrogen-doped ultra-microporous carbons as efficient contenders for CO2 capture. *Chem. Eng. J.* **2018**, *352*, 539−548.